

Investigating Temporal Control in Photoinduced Atom Transfer Radical Polymerization

Sajjad Dadashi-Silab,[¶] In-Hwan Lee,[¶] Athina Anastasaki,^{*} Francesca Lorandi, Benjaporn Narupai, Neil D. Dolinski, Michael L. Allegrezza, Marco Fantin, Dominik Konkolewicz, Craig J. Hawker,^{*} and Krzysztof Matyjaszewski^{*}



Cite This: *Macromolecules* 2020, 53, 5280–5288



Read Online

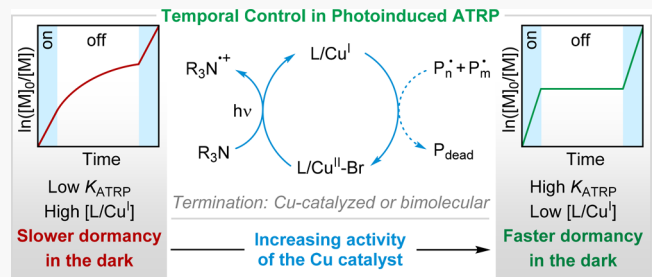
ACCESS |

Metrics & More

Article Recommendations

Supporting Information

ABSTRACT: External regulation of controlled polymerizations allows for controlling the kinetics of the polymerization and gaining spatial or temporal control over polymer growth. In photoinduced atom transfer radical polymerization (ATRP), light irradiation (re)generates the copper catalyst to switch the polymerization on. However, removing the light does not immediately inactivate the catalyst, nor does the rate of polymerization become zero as chains may grow in the dark because of continued activation by the residual activator catalyst or regeneration of the Cu catalyst in the dark. In this paper, the effect of polymerization components on photoinduced ATRP was investigated to understand the interplay of temporal control and light switching. Kinetics of polymerization were monitored using *in situ* NMR as well as under conventional batch conditions. The extent of the polymerization in the dark depended on the activity of the Cu catalyst, which was regulated by the nature of the ligand and reaction medium. For highly active catalysts, the equilibrium concentration of the L/Cu^I activator is very low, and it was rapidly depleted by radical termination reactions, yielding temporal control which closely matched the switching of light to on or off. Decreasing the activity of the Cu catalyst increased the equilibrium concentration of the activator, leading to significant chain growth in the dark.



INTRODUCTION

Stimuli-responsive catalytic systems can be modulated by external factors such as heat, light, or electrochemical potential to alter their properties and function in catalyzing and controlling the rate and selectivity of chemical reactions.¹ In controlled polymerization techniques, external regulation has provided new opportunities to synthesize advanced polymers and expand understanding of underlying mechanisms.^{2–4}

Tied to these catalytic systems, photochemistry has been extensively used for chemical transformations.⁵ Application of photochemistry in controlled polymerization techniques^{6–8} such as atom transfer radical polymerization (ATRP),^{9–19} photoinduced electron/energy transfer in reversible addition–fragmentation chain transfer,^{20–24} cationic,^{25,26} ring-opening,²⁷ and ring-opening metathesis polymerizations²⁸ has led to significant advancements in polymer synthesis and enabled spatial and temporal control over polymerization.

ATRP^{29,30} can be efficiently carried out with minute amounts of Cu catalysts using various activator (re)generation techniques.^{31–33} For example, ATRP has been performed using zerovalent metals,^{34–38} radical initiators,³⁹ reducing agents,^{40,41} and photo-,^{8,17,18,42–45} electro-,^{46–49} and mechano-chemical stimuli.^{50–53} A common feature of these ATRP initiating systems is the (re)generation of the activator

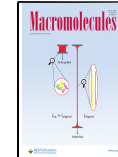
L/Cu^I species via reduction of the deactivator, $L/Cu^{II}-Br$, which is used initially and is accumulated throughout polymerization because of unavoidable radical terminations.

The use of external stimuli provides temporal control over ATRP through modulating the oxidation state of the Cu catalyst.^{4,46,54} In the case of photoinduced ATRP, light is used to promote the reaction of the $L/Cu^{II}-Br$ deactivator in the excited state with electron donors such as amines.⁴³ However, upon removal of the external stimulus, the remaining L/Cu^I activator in solution can often lead to further chain growth.^{52,55–57} In photocontrolled polymerizations, the growth of polymer chains depends on continuous light irradiation, during which chain growth is enabled by photochemical electron- or energy-transfer reactions by photo-excited-state catalysts. Consequently, temporal control can be efficiently achieved upon applying or removing light while maintaining control over polymerization. In Cu-catalyzed photoinduced

Received: April 16, 2020

Revised: May 20, 2020

Published: June 16, 2020



ATRP, chain ends are activated by the L/Cu^I activator in the ground state, and switching light off stops the regeneration of the activator catalyst. However, polymer chains may continue to grow further in the dark as a result of the presence of the residual L/Cu^I activator in solution, which is regulated by the ATRP equilibrium between the L/Cu^I and $L/Cu^{II}-Br$ species. The extent of polymerization in the absence of external stimuli depends on the relative concentration of L/Cu^I and $L/Cu^{II}-Br$, which is determined by the nature of the catalyst/ligand, reaction medium, and (re)generation mechanism.^{58–60} Highly active catalysts shift the ATRP equilibrium toward a low concentration of L/Cu^I , whereas with less active catalysts, a higher concentration of L/Cu^I in solution may continue polymerization without stimuli. Accordingly, temporal control in ATRP using Cu catalysts depends, among other factors, on the activity and concentration of the catalyst.^{55–57,61,62}

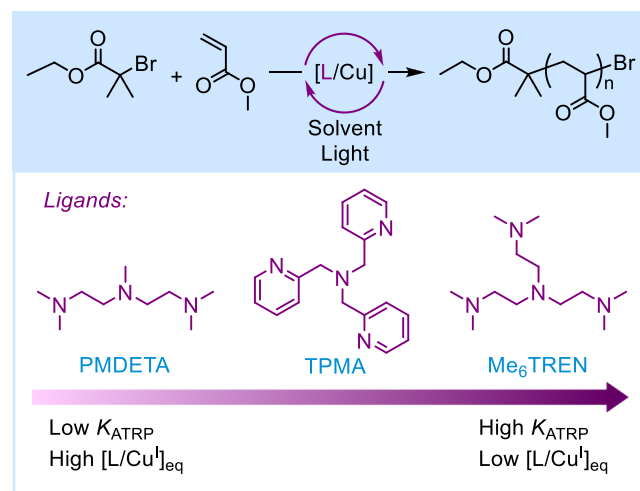
ATRP is subject to the persistent radical effect, where unavoidable radical termination processes consume the activator and lead to a buildup of the deactivator.⁶³ As a consequence, the rate of polymerization decreases over time, and the consumption of the L/Cu^I activator causes the polymerization to pause. However, use of oxidizing external stimuli offers a more efficient way to pause the polymerization while preserving high chain-end functionality for subsequent restarting of the polymerization under reducing stimuli. Indeed, switching the oxidation state of the Cu catalyst with external stimuli offers switching polymerization on demand between on and off states.^{46,54}

This paper investigates temporal control in photoinduced ATRP and examines how the nature and activity of the Cu catalyst with different ligands or the reaction medium impacts the response of the polymerization to switching the light on/off. Significantly, highly active catalytic systems were shown to enable excellent temporal control through multiple on/off light switches with minimal polymerization observed in the dark periods. In the absence of light, radical termination reactions consume the low concentration of the activator present, stopping the polymerization. However, when using catalysts with lower activity, the polymerization continued in the dark because of the presence of a relatively high concentration of the ATRP activator when the light was switched off. Significantly improved temporal control was attained with less active catalytic systems by using oxygen to oxidize the residual L/Cu^I activator.

RESULTS AND DISCUSSION

Temporal control in photoinduced ATRP was investigated in the polymerization of methyl acrylate (MA) using *N,N,N',N'',N''*-pentamethyldiethylenetriamine (PMDETA), tris(2-pyridylmethyl)amine (TPMA), and tris[2-(dimethylamino)ethyl]amine (Me_6TREN) ligands (Scheme 1). The choice of the ligand and reaction medium allows for tuning the activity of the Cu catalyst and hence the kinetics of the polymerization.⁶⁰ The activity of the Cu catalyst in ATRP increases when the ligand is changed from PMDETA to TPMA and to Me_6TREN .⁶⁴ Therefore, temporal control in photoinduced ATRP was studied using different ligands and solvents to examine their effect on the polymerization behavior in response to photochemical switching. To minimize potential experimental errors, real-time optical fiber-coupled 1H NMR monitoring⁶⁵ was applied in addition to conventional batch conditions. Specifically, polymerization of MA was performed in an NMR tube equipped with the optical fiber on top of the

Scheme 1. Photoinduced ATRP in the Presence of Different Ligands Promoting Different Catalytic Activity; Ligands: PMDETA, TPMA, and Me_6TREN



sample, and the reaction was monitored with intermittent on/off cycles (cf. Supporting Information).

To begin temporal control studies, a series of in situ experiments using Me_6TREN were carried out under fixed conditions. Polymerization of MA (50 equiv) was performed with 0.02 equiv of copper(II) bromide ($CuBr_2$), 0.12 equiv of Me_6TREN , and 1 equiv of ethyl α -bromo isobutyrate (EBiB) as the initiator in deuterated dimethyl sulfoxide ($DMSO-d_6$) under irradiation with 405 nm light-emitting diodes (LEDs). Kinetic analysis revealed rapid polymerization, reaching 63% conversion after 30 min. Then, the light was turned off, and the reaction was monitored in the dark for an extended time period. Without light exposure, the rate of polymerization was lower and gradually decreased with time. However, the polymerization never ceased, ultimately reaching 93% monomer conversion after 12 h (Figure 1A). This result strongly suggests that the activator complex, L/Cu^I , continuously drove the polymerization through the dark period. Importantly, similar behavior was observed for the attempted temporal control of MA polymerization under conventional batch conditions. Significant chain growth occurs over an extended period after removal of the light (Figures 1B and S1). As a

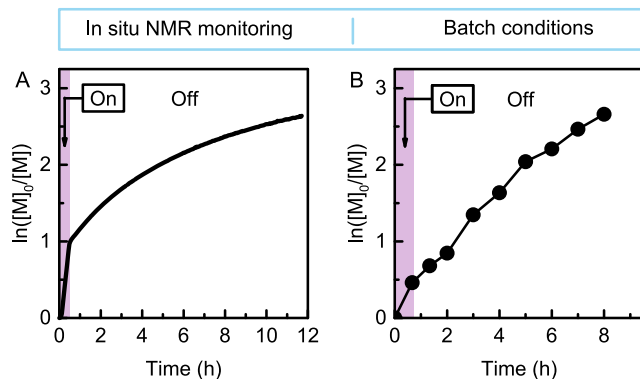


Figure 1. Temporal control in photoinduced ATRP demonstrating continued chain growth in the dark monitored (A) via in situ NMR or (B) under conventional batch conditions. Reaction conditions: $[MA]/[EBiB]/[CuBr_2]/[Me_6TREN] = 50/1/0.02/0.12$ in $DMSO$ ($[MA] = 5.5 \text{ M}$).

result, it is necessary to identify the contribution of polymerization components, such as the reaction medium and the concentration of the Cu catalyst and ligand, on the chain growth in the dark. The ultimate goal is to identify conditions for improving temporal control in photoinduced ATRP.

Control experiments performed in the dark showed that polymerization of MA could be initiated without light irradiation. For example, under typical conditions with a target degree of polymerization (DP) of 50 using 0.12 equiv of Me_6TREN in DMSO, polymerization of MA reached 92% monomer conversion in 24 h in the dark (no exposure to ambient light). These results suggest that the $\text{L}/\text{Cu}^{\text{I}}$ activator is generated in the dark in the presence of Me_6TREN , which could then act as a reducing agent for $\text{L}/\text{Cu}^{\text{II}}-\text{Br}$ and/or as an activator of the alkyl halide initiator to generate initiating radicals in the dark. Similar observations were reported when using alkyl amine-containing compounds such as PMDETA or 2-(dimethylamino)ethyl methacrylate as reducing agents.^{66,67}

Effect of Concentration of the Ligand and Cu Catalyst on Temporal Control in Photoinduced ATRP.

To investigate the effect of excess of the ligand relative to Cu loading, the concentration of Me_6TREN was systematically decreased to reduce the rate of regeneration of the $\text{L}/\text{Cu}^{\text{I}}$ activator, thus suppressing polymerization during the dark period. In the presence of 0.02 equiv of CuBr_2 , the amount of Me_6TREN was gradually reduced from 0.12 to 0.06 and to 0.04 equiv (relative to the initiator, which corresponds to 6, 3, and 2 times, respectively, vs CuBr_2) and was tested through three on/off cycles (each on/off period is 30 min; Table 1,

Table 1. Reactivity and On/Off Control of Polymerizations Depending on the Concentrations of CuBr_2 and Me_6TREN ^a

entry	CuBr_2 (equiv)	Me_6TREN (equiv)	conv. (%)	M_n	\mathcal{D}	$k_{\text{off}}/k_{\text{on}}$		
						1st	2nd	3rd
1	0.02	0.12	94	5300	1.08	0.18	0.23	0.26
2	0.02	0.06	93	4400	1.10	0.08	0.09	0.08
3	0.02	0.04	91	4200	1.11	0.07	0.07	0.03
4	0.01	0.12	95	4100	1.15	0.11	0.19	0.23
5	0.005	0.12	93	3400	1.27	0.10	0.18	0.22
6	0.005	0.015	87	4100	1.16	0.05	0.0	0
7	0.005	0.010	75	3000	1.26	0.05	0.02	0.12

^aReactions were performed under in situ NMR monitoring. Molecular weight properties were obtained using size exclusion chromatography (SEC) in chloroform with polystyrene standards.

entries 1–3). Upon decreasing the amount of Me_6TREN from 0.12 to 0.06 and to 0.04 equiv, the ratio of the apparent propagation rate constants in the light-off and light-on periods ($k_{\text{off}}/k_{\text{on}}$) for the first cycle gradually decreased from 0.18 to 0.08 and to 0.07, respectively (Table 1, entries 1–3), indicating enhanced temporal control in the presence of a low concentration of Me_6TREN . Importantly, polymerizations reached a high monomer conversion (>90%) with number-average molecular weights (M_n) of 4200–5300 and low dispersity values ($\mathcal{D} \approx 1.08$ –1.11), suggesting well-controlled polymerizations under all conditions (Table 1, entries 1–3).

The effect of catalyst loading was then investigated by systematically reducing the concentration of CuBr_2 from 0.02 to 0.005 equiv (with respect to the initiator) while keeping the amount of Me_6TREN constant at 0.12 equiv (Table 1, entries

1, 4, and 5). On decreasing the amount of CuBr_2 from 0.02 to 0.005 equiv, k_{off} decreased by a factor of ~2 from 18 to 10% of the respective k_{on} values (Table 1, entries 1, 4, and 5), indicating improved temporal control. Polymerizations were well-controlled with high monomer conversions (93–95%) and low \mathcal{D} values (1.08–1.27). Accordingly, the polymerization of MA was carried out with reduced concentrations of both CuBr_2 and Me_6TREN to synergistically achieve low $k_{\text{off}}/k_{\text{on}}$ values. Polymerization with 0.005 equiv of CuBr_2 and 0.015 equiv of Me_6TREN (4 and 8 times less than the corresponding amounts used under standard conditions) showed excellent temporal control ($k_{\text{off}}/k_{\text{on}} = 0.05$ for the first cycle) while maintaining a high monomer conversion (87%) and resulting in polymers with a low \mathcal{D} of 1.16 (Table 1, entry 6). Further decreasing the concentration of Me_6TREN to 0.01 equiv resulted in a similar enhancement of temporal control ($k_{\text{off}}/k_{\text{on}} = 0.05$ for the first cycle). However, the rate of polymerization decreased (75% conversion after three cycles), and the third cycle showed an inferior response when the light was switched off. Additionally, the resulting polymer showed a higher \mathcal{D} than the case of 0.015 equiv of Me_6TREN (1.26 vs 1.16; Table 1, entries 6 and 7, and Figure 2). These results indicated that

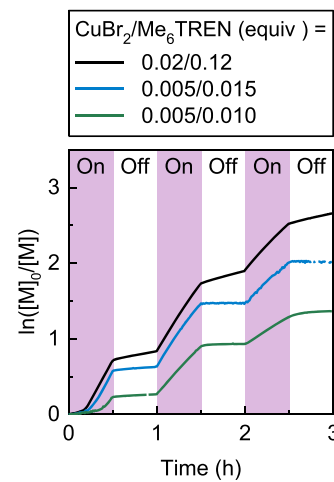


Figure 2. Effect of decreasing concentration of CuBr_2 and Me_6TREN on kinetics of temporal control in photoinduced ATRP of MA. Reaction conditions: $[\text{CuBr}_2]/[\text{Me}_6\text{TREN}] = 0.02/0.12$, 0.005/0.015, or 0.005/0.010 corresponding to entries 1, 6, and 7, respectively, in Table 1, kinetics monitored by in situ NMR.

polymerization can be efficiently controlled even with diminished concentrations of the catalyst. Decreasing the concentration of CuBr_2 and the ligand decreased the equilibrium concentration of $\text{L}/\text{Cu}^{\text{I}}$, thereby resulting in an enhanced temporal response.

Effect of Solvents on Temporal Control in Photoinduced ATRP. Based on the optimized reaction conditions in DMSO, two additional deuterated solvents including acetonitrile (CD_3CN) and methanol (MeOD), which show different reactivities in ATRP,⁶⁸ were chosen to study the effect of solvents using in situ NMR monitoring. Polymerizations were performed using CuBr_2 (0.01 equiv) and Me_6TREN (0.06 equiv). The $k_{\text{off}}/k_{\text{on}}$ values for the first cycle were 0.04 and 0.11 in MeOD and CD_3CN , respectively, demonstrating good temporal control (Figure S2).

Reducing the concentration of CuBr_2 to 0.005 equiv in the presence of 0.015 equiv of Me_6TREN resulted in enhanced

temporal control ($k_{\text{off}}/k_{\text{on}}$ values down to 0.02 and 0.09 in MeOD and CD₃CN, respectively), without compromising control over the polymerization process (Figure 3). Thus, the

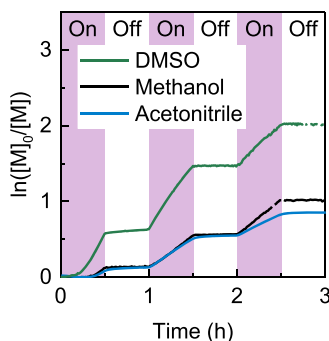


Figure 3. Temporal control of photoinduced ATRP in different solvents, followed by in situ NMR monitoring using CuBr₂ (0.005 equiv) and Me₆TREN (0.015 equiv). $k_{\text{off}}/k_{\text{on}}$ values of the first/second/third cycles are 0.02/0.03/0.02 in methanol or 0.09/0.04/0.04 in acetonitrile, respectively.

stoichiometric adjustment of the catalytic system resulted in enhanced temporal regulation in both solvents, proving a general strategy to improve temporal control in photoinduced ATRP.

Similarly, under batch conditions, changing the solvent from DMSO to MeCN or DMF resulted in limited chain growth in the dark with the rate of the polymerization decreasing over time and eventually stopping (Figure 4). Re-exposing the

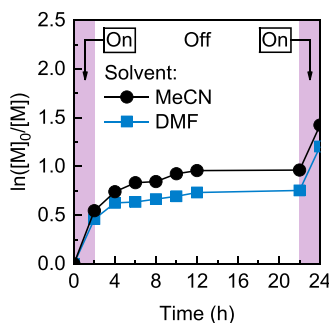


Figure 4. Temporal control in photoinduced ATRP of MA using MeCN and DMF as solvents. Reaction conditions: [MA]/[EBiB]/[CuBr₂]/[Me₆TREN] = 50/1/0.02/0.12 in 50 vol% solvent (MeCN or DMF, [MA] = 5.5 M), irradiated with violet LEDs ($\lambda_{\text{max}} = 394$ nm, 2.6 mW/cm²) under batch conditions.

solutions to light reinitiated the polymerizations with higher monomer conversions and well-controlled polymerizations being observed (Figure S3). Furthermore, control experiments performed in the dark with a target DP of 50 showed no polymerization in DMF after keeping the reaction mixture in the dark for 90 h. In MeCN, a slow polymerization of MA was observed in the dark with ~57% monomer conversion obtained in 90 h, showing an induction period >24 h. These results suggest that in the presence of tertiary amines as a reducing agent, progression of the polymerization is more pronounced in DMSO than in MeCN or DMF because of the higher K_{ATRP} in DMSO.⁶⁸

Effect of Activity of the Cu Catalyst on Temporal Control in Photoinduced ATRP. The activity of the Cu catalyst in ATRP can also be tuned using different ligands,

enabling a dynamic modulation of the molar ratio of the activator and deactivator species. Temporal control in the photoinduced ATRP of MA (target DP = 200) in the presence of 0.02 equiv of CuBr₂ using Me₆TREN, TPMA, and PMDETA ligands (0.12 equiv) in DMSO was then examined under conventional batch conditions. Excellent temporal control was achieved in photoinduced ATRP of MA using Me₆TREN as a ligand. As shown in Figure 5A, temporal control was achieved upon intermittent light on/off periods for 20 min with low monomer conversion being observed during the dark periods. Importantly, no significant chain growth is apparent when the light was removed for a longer time period—80 min (Figure 5B). Re-exposing the solutions to light restarted the polymerizations in a controlled manner, yielding polymers with molecular weights in agreement with theoretical values and low $D < 1.1$ (Figure S4).

The higher ATRP activity of the Cu complex with Me₆TREN results in a larger ATRP equilibrium constant, K_{ATRP} ,⁶⁹ and increases the ratio of the concentration of the L/Cu^{II}–Br deactivator to the concentration of the L/Cu^I activator under equilibrium. This higher value of K_{ATRP} results in a lower concentration of L/Cu^I during the polymerization.⁵⁸ Upon removal of the light, the low concentration of residual L/Cu^I was rapidly consumed by radical termination reactions, converting L/Cu^I to L/Cu^{II}–Br and therefore stopping the polymerization.

In contrast, when using TPMA as the ligand in DMSO, the polymerization responded slowly to switching the light off, leading to poor temporal control. Figure 5C shows that the polymerization continued in dark periods with rates similar to those under light irradiation. However, as shown in Figure 5D, when the reaction was kept in the dark for 4 h, chain growth was observed only in the first hour, and subsequently, the polymerization rate decreased. Re-exposing the solution to light restarted the polymerization in a controlled way (Figures S5 and S6). From these studies, it can be concluded that the Cu catalyst with the TPMA ligand is less active compared to Me₆TREN; therefore, the equilibrium concentration of L/Cu^I with TPMA was higher, resulting in chain growth during dark periods.

Significant chain growth was observed in dark periods when PMDETA was used as the ligand. As presented in Figure 5E, polymerization with PMDETA showed essentially no response to switching the light off, and a linear kinetic behavior was obtained regardless of the light being on or off. Moreover, significant monomer conversion was observed even when the reaction was kept in the dark for longer periods (Figure 5F). The polymerization was started by irradiating the solution with violet LEDs, yielding 27% monomer conversion within 4 h. Afterward, the solution was kept in the dark for 16 h. Interestingly, the polymerization continued during this period, reaching 82% monomer conversion. A decrease in the polymerization rate was observed only toward the end of the dark period (Figure 5F). Importantly, these polymerizations undergoing significant chain growth in the dark were still well-controlled, giving polymers with molecular weights in agreement with theoretical values and a low D of 1.10 (Figures S7 and S8). Analysis of these results shows that PMDETA forms a Cu complex with a lower catalytic activity compared to both TPMA and Me₆TREN,⁶⁴ resulting in a lower rate of polymerization and hence lower concentration of radicals. In addition, the low activity of the catalyst determined a relatively high concentration of L/Cu^I, and therefore, the polymerization

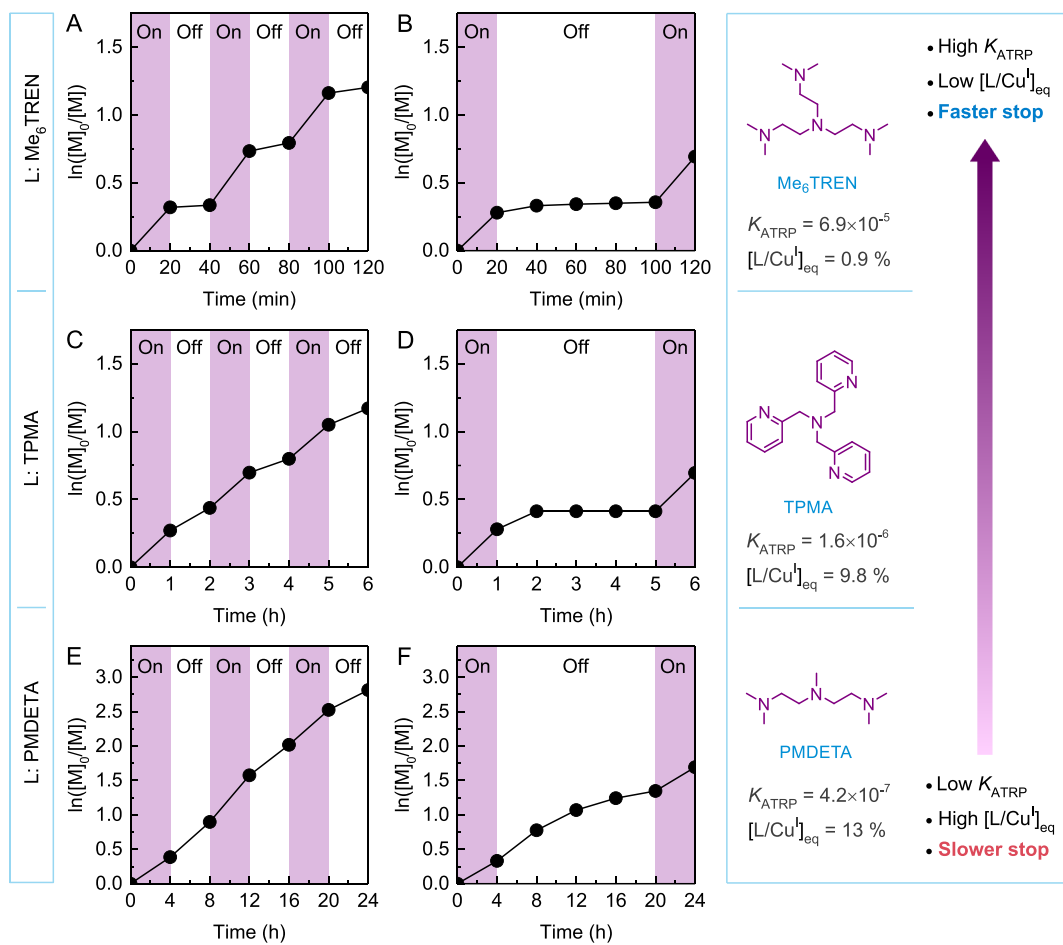


Figure 5. Temporal control in photoinduced ATRP of MA using Me_6TREN (A, B), TPMA (C, D), and PMDETA (E, F) ligands, demonstrating dependency on the activity of the Cu catalyst as a result of the nature of the ligand. Reaction conditions: $[\text{MA}]/[\text{EBiB}]/[\text{CuBr}_2]/[\text{L}] = 200/1/0.02/0.12$ (for TPMA, $\text{L} = 0.02$, triethylamine = 0.4 equiv) in 50 vol% DMSO ($[\text{MA}] = 5.5 \text{ M}$). Irradiated with violet LEDs ($\lambda_{\text{max}} = 394 \text{ nm}$, 2.6 mW/cm^2) under batch conditions.

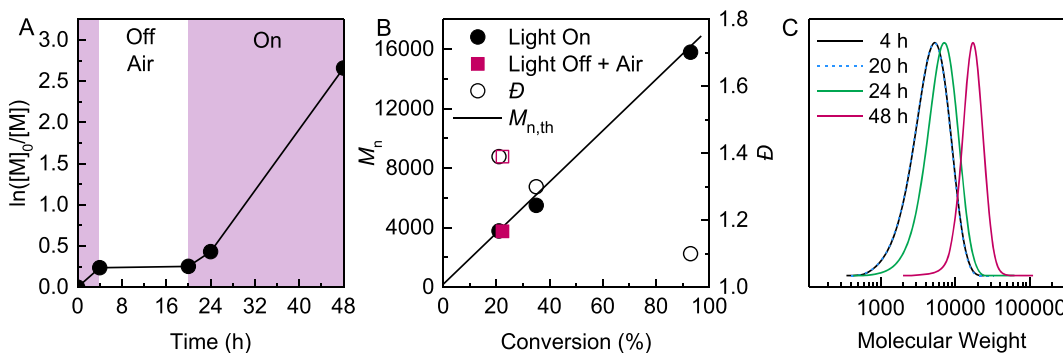


Figure 6. Temporal control in photoinduced ATRP of MA using oxygen as an oxidizing stimulus to stop the polymerization in the dark in the presence of PMDETA. Reaction conditions: $[\text{MA}]/[\text{EBiB}]/[\text{CuBr}_2]/[\text{PMDETA}] = 200/1/0.02/0.12$ in 50 vol% DMSO ($[\text{MA}] = 5.5 \text{ M}$). Irradiation with violet LEDs ($\lambda_{\text{max}} = 394 \text{ nm}$, 2.6 mW/cm^2) under batch conditions.

continued to high monomer conversions without the need for light-induced activator (re)generation.

Consuming the $\text{L}/\text{Cu}^{\text{I}}$ catalyst via external stimuli would improve temporal control in the presence of the PMDETA ligand. Oxygen was successfully used as an oxidizer to switch the Cu catalyst off and achieve temporal control with PMDETA. The polymerization was started upon light irradiation, giving 22% monomer conversion in 4 h. The light was then switched off, and the solution was bubbled with

air for 1 min. The Cu catalyst was switched off upon oxidation with oxygen, and no polymerization was observed in the subsequent dark period. Re-exposing the solution to light restarted the polymerization with the monomer conversion reaching 35% within 4 h (Figure 6). The polymerization then reached a high monomer conversion under continuous light irradiation (final conversion = 93%) with SEC analysis revealing narrow, symmetric distribution of molecular weights and a low \mathcal{D} ($M_n = 15,800$, $M_{n,\text{th}} = 16,200$, $\mathcal{D} = 1.11$), all in

Table 2. Thermodynamic and Kinetic Parameters of ATRP for Various Cu Catalysts Measured on an RDE^a

ligand	$E^\theta_{(L/Cu^{II}-Br)/(L/Cu^I)}$ (V vs SCE)	K_{ATRP}	$k_{act} (M^{-1} s^{-1})^b$	$k_{deact} (M^{-1} s^{-1})$	$[R^\bullet] (M)$	$[L/Cu^I] (mM)$	$[L/Cu^I] (\%)$
Me ₆ TREN	-0.297	6.9×10^{-5}	3.8×10^3	5.6×10^7	1.70×10^{-8}	0.0048	0.9
TPMA	-0.159	1.6×10^{-6}	60	3.8×10^7	4.81×10^{-9}	0.0541	9.8
PMDETA	-0.113	4.2×10^{-7}	1.6	3.8×10^6	1.71×10^{-9}	0.0710	13

^aConditions: 0.1 M Et₄NBF₄, $T = 25$ °C in MA/DMSO (1/1). For determination of K_{ATRP} : $[L/Cu^I] = 0.5$ mM, [MBP] = 50 mM (for L = Me₆TREN, [MBP] = 25 mM), and RDE rotation = 2500 rpm. ^bFor determination of k_{act} : $[L/Cu^I] = 0.5$ mM, [MBP] = 0.5 mM (for L = PMDETA, [MBP] = 10 mM), [TEMPO] = 50 mM, RDE rotation = 4000 rpm, and $k_p = 1.5 \times 10^4$ ($M^{-1} s^{-1}$).⁷¹ MBP: methyl 2-bromopropionate.

agreement with theoretical values and a well-controlled process. This result confirms that excellent temporal control in ATRP can be achieved even in low-activity catalytic systems by applying dual stimuli to switch the polymerization off by oxidation of L/Cu^I. Importantly, introduction of oxygen as an oxidizing agent did not result in loss of control over the polymerization, indicating the tolerance of this system in the presence of small amounts of oxygen due to a very fast reaction of oxygen with L/Cu^I, which is present at a much higher concentration than the radical chain end of the growing polymer chains.

Electrochemical Analysis of the Cu Catalysts Used in Temporal Control. The concentration of L/Cu^I present at the end of the first light-on period was estimated according to eq 1. Assuming steady-state conditions, the relative ratio of $[L/Cu^I]/[L/Cu^{II}-Br]$ can be expressed as

$$\frac{[L/Cu^I]}{[L/Cu^{II}-Br]} = \left(\frac{1}{K_{ATRP}} \right) \left(\frac{[R^\bullet]}{[R-Br]} \right) \quad (1)$$

In well-controlled radical polymerizations, only a small fraction of chains undergoes radical termination; therefore, $[R-X]$ can be assumed to be equal to its initial concentration, $[R-X]_0$, while $[R^\bullet]$ can be calculated from the slope of the semilogarithmic kinetic plot as $[R^\bullet] = \text{slope}/k_p$, where k_p is the propagation rate constant. Table 2 shows the values of K_{ATRP} , the rate constants of activation (k_{act}) and deactivation (k_{deact}), and the concentration of radicals and L/Cu^I for the three ligands studied in temporal control experiments. The values of K_{ATRP} and k_{act} in the MA/DMSO mixture were determined by chronoamperometry on a rotating disk electrode (RDE) according to previously reported procedures.^{69,70} The k_{deact} values were calculated as k_{deact}/K_{ATRP} .

The values presented in Table 1 show that on decreasing the activity of the Cu catalyst and hence the K_{ATRP} value, the concentration of L/Cu^I increases. For example, for Me₆TREN as a ligand, ~0.9% of the total catalyst was calculated to be in the L/Cu^I form, whereas for TPMA, this value was ~9.8, and for PMDETA, this value was ~13%.

As radical termination reactions consume the L/Cu^I activator to form the L/Cu^{II}-Br deactivator, according to the persistent radical effect, in the absence of light or any other activator (re)generator, the consumption of the activator by terminations leads the polymerization to slow down and ultimately stop.⁶³ Considering the concentration of L/Cu^I activators in Table 2, the extent of radical termination needed to consume all L/Cu^I was estimated for the different catalysts. For example, in the presence of Me₆TREN, 0.88% of the total Cu catalyst was calculated to be present as L/Cu^I. With the initial concentration of the catalyst being 2 mol% of $[RX]_0$, termination of only 0.017% of chains would lead to the

consumption of all residual L/Cu^I. Similarly, in the presence of the TPMA and PMDETA ligands, all residual L/Cu^I could be consumed upon termination of 0.19 and 0.25% of the total chains, respectively. These results agree with the experimental observation that highly active catalysts show a quicker response to switching the light off, therefore offering better temporal control because less termination is required to consume L/Cu^I. Importantly, in each case, the chains terminating during the dark periods were a tiny fraction of the living chains.

In the ATRP of acrylate monomers, radical termination reactions can occur through different pathways including conventional radical termination and catalyzed radical termination (CRT) reactions.^{60,72} As presented in Figure 7A (pink lines), conventional radical termination involves a bimolecular reaction of radicals consuming one molecule of the L/Cu^I activator per each terminating radical. In addition, radicals can terminate through the CRT mechanism (blue lines, Figure 7A). CRT involves the reaction of L/Cu^I with a propagating radical to form an organometallic intermediate, L/P_n-Cu^{II}. Although the exact mechanism of CRT is still under investigation, it has been proposed that the interaction between a propagating chain and the paramagnetic organometallic species leads to terminated chains and regeneration of L/Cu^I.⁷³ In the overall mass balance of ATRP and CRT, one molecule of L/Cu^I is consumed per each terminating radical.

Simulations using the PREDICI software⁷⁴ were therefore performed to quantify the behavior of the polymerization systems in the dark, when no activator (re)generation occurs. In addition, simulations were based on TPMA as the ligand because of the available data on the formation of TPMA/P_n-Cu^{II} intermediates⁷⁵ according to the model shown in Scheme S1. Interestingly, simulations involving only the conventional radical termination pathway showed a slow consumption of TPMA/Cu^I, resulting in increasing monomer conversion in the dark (Figure 7B, blue line). However, a more accurate agreement with experimental data was obtained when including both conventional radical termination and CRT pathways in the simulations. CRT promoted a more rapid consumption of L/Cu^I, thus favoring a faster decrease in the rate of polymerization. The best agreement between experimental and simulated data was obtained with the rate constant of CRT $k_{CRT} = 10^8$ $M^{-1} s^{-1}$. This value is higher than recently measured for the Cu/TPMA system in dry DMSO,⁷⁵ suggesting that additional termination pathways can contribute in this polymerization system, arising from the presence of residual water or other impurities.⁷⁶

CONCLUSIONS

Temporal control in photoinduced ATRP processes was investigated to understand the fundamental behavior of ATRP systems in the dark. Conditions were identified for

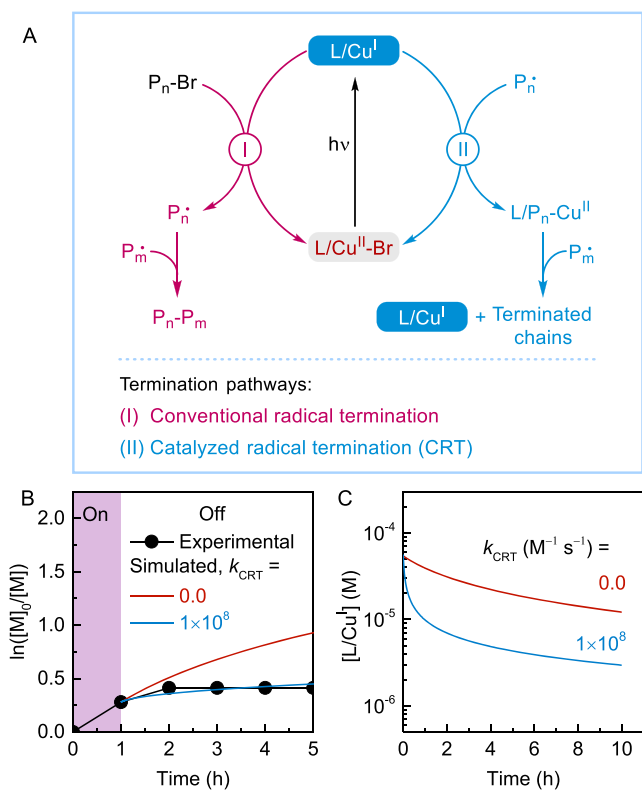


Figure 7. (A) Termination of radicals in ATRP: (I) pink lines represent conventional radical termination and (II) blue lines represent catalyzed radical termination (CRT). For each radical terminated, one molecule of $L/Cu^{I\cdot}$ is converted to L/Cu^{II-Br} . (B) Overlay of experimental (shown in black) and simulated kinetic results in the dark periods for the polymerization with $L = \text{TPMA}$, considering only bimolecular radical termination (shown in red) or bimolecular radical termination and CRT (shown in blue). (C) Evolution of $[L/Cu^{I\cdot}]$, where $L = \text{TPMA}$ in the dark (no activator regeneration) as simulated by PREDICI considering only bimolecular radical termination (shown in red) or bimolecular radical termination and CRT (in blue). Initial reaction conditions: $[\text{MA}]/[\text{EBiB}]/[\text{CuBr}_2]/[\text{TPMA}] = 200/1/0.02/0.12$ in 50 vol% DMSO ($[\text{MA}] = 5.5 \text{ M}$).

improved temporal control over photoinduced ATRP by studying the effect of reaction components including the catalyst, ligand, and solvent. The activity of the catalyst regulates the molar ratio between the $L/Cu^{I\cdot}$ activator and the L/Cu^{II-Br} deactivator, resulting in a decrease in the concentration of $L/Cu^{I\cdot}$ as the activity of the catalyst increases. Excellent temporal control was achieved with Me_6TREN , which forms a highly active Cu catalyst, whereas chain growth in the dark was observed in the presence of the TPMA or PMDETA ligand. It is noted that these catalyst systems have lower activity compared to Me_6TREN . The results of temporal control in photoinduced ATRP illustrate the importance of tuning the activity of the Cu catalyst by modifying the concentration and nature of the ligand and the reaction medium to achieve enhanced temporal control in Cu-catalyzed ATRP. The findings of this work provide a general guideline for understanding how Cu-based catalytic systems behave in externally controlled ATRP and designing better catalysts for gaining efficient temporal control over polymerizations.

ASSOCIATED CONTENT

SI Supporting Information

The Supporting Information is available free of charge at <https://pubs.acs.org/doi/10.1021/acs.macromol.0c00888>.

Experimental procedures and detailed kinetics and polymerization results (PDF)

AUTHOR INFORMATION

Corresponding Authors

Athina Anastasaki — Materials Research Laboratory, University of California, Santa Barbara, California 93106, United States; orcid.org/0000-0002-6615-1026; Email: athina.anastasaki@mat.ethz.ch

Craig J. Hawker — Materials Research Laboratory, Department of Chemistry and Biochemistry, and Materials Department, University of California, Santa Barbara, California 93106, United States; orcid.org/0000-0001-9951-851X; Email: hawker@mrl.ucsb.edu

Krzysztof Matyjaszewski — Department of Chemistry, Carnegie Mellon University, Pittsburgh, Pennsylvania 15213, United States; orcid.org/0000-0003-1960-3402; Email: km3b@andrew.cmu.edu

Authors

Sajjad Dadashi-Silab — Department of Chemistry, Carnegie Mellon University, Pittsburgh, Pennsylvania 15213, United States; orcid.org/0000-0002-4285-5846

In-Hwan Lee — Materials Research Laboratory, University of California, Santa Barbara, California 93106, United States; Department of Chemistry, Ajou University, Suwon 16499, Korea; orcid.org/0000-0002-4848-939X

Francesca Lorandi — Department of Chemistry, Carnegie Mellon University, Pittsburgh, Pennsylvania 15213, United States; orcid.org/0000-0001-5253-8468

Benjaporn Narupai — Materials Research Laboratory, University of California, Santa Barbara, California 93106, United States

Neil D. Dolinski — Materials Research Laboratory and Materials Department, University of California, Santa Barbara, California 93106, United States

Michael L. Allegrezza — Department of Chemistry and Biochemistry, Miami University, Oxford, Ohio 45056, United States

Marco Fantin — Department of Chemistry, Carnegie Mellon University, Pittsburgh, Pennsylvania 15213, United States

Dominik Konkolewicz — Department of Chemistry and Biochemistry, Miami University, Oxford, Ohio 45056, United States; orcid.org/0000-0002-3828-5481

Complete contact information is available at: <https://pubs.acs.org/10.1021/acs.macromol.0c00888>

Author Contributions

[¶]S.D.-S. and I.-H.L. contributed equally.

Notes

The authors declare no competing financial interest.

ACKNOWLEDGMENTS

Financial support from NSF (CHE 1707490 and CHE 2000391) and partial support by the National Science Foundation (NSF) through the Materials Research Science and Engineering Center at UC Santa Barbara, DMR-1720256 (IRG-3), are gratefully acknowledged.

■ REFERENCES

(1) Blanco, V.; Leigh, D. A.; Marcos, V. Artificial switchable catalysts. *Chem. Soc. Rev.* **2015**, *44*, 5341–5370.

(2) Leibfarth, F. A.; Mattson, K. M.; Fors, B. P.; Collins, H. A.; Hawker, C. J. External Regulation of Controlled Polymerizations. *Angew. Chem., Int. Ed.* **2013**, *52*, 199–210.

(3) Teator, A. J.; Lastovickova, D. N.; Bielawski, C. W. Switchable Polymerization Catalysts. *Chem. Rev.* **2016**, *116*, 1969–1992.

(4) Pan, X.; Fantin, M.; Yuan, F.; Matyjaszewski, K. Externally controlled atom transfer radical polymerization. *Chem. Soc. Rev.* **2018**, *47*, 5457–5490.

(5) Stephenson, C.; Yoon, T.; MacMillan, D. W. C. *Visible Light Photocatalysis in Organic Chemistry*; Wiley-VCH, 2018.

(6) Chen, M.; Zhong, M.; Johnson, J. A. Light-Controlled Radical Polymerization: Mechanisms, Methods, and Applications. *Chem. Rev.* **2016**, *116*, 10167–10211.

(7) Dadashi-Silab, S.; Doran, S.; Yagci, Y. Photoinduced Electron Transfer Reactions for Macromolecular Syntheses. *Chem. Rev.* **2016**, *116*, 10212–10275.

(8) Pan, X.; Tasdelen, M. A.; Laun, J.; Junkers, T.; Yagci, Y.; Matyjaszewski, K. Photomediated controlled radical polymerization. *Prog. Polym. Sci.* **2016**, *62*, 73–125.

(9) Fors, B. P.; Hawker, C. J. Control of a Living Radical Polymerization of Methacrylates by Light. *Angew. Chem., Int. Ed.* **2012**, *51*, 8850–8853.

(10) Anastasaki, A.; Nikolaou, V.; Zhang, Q.; Burns, J.; Samanta, S. R.; Waldron, C.; Haddleton, A. J.; McHale, R.; Fox, D.; Percec, V.; Wilson, P.; Haddleton, D. M. Copper(II)/Tertiary Amine Synergy in Photoinduced Living Radical Polymerization: Accelerated Synthesis of ω -Functional and α,ω -Heterofunctional Poly(acrylates). *J. Am. Chem. Soc.* **2014**, *136*, 1141–1149.

(11) Theriot, J. C.; McCarthy, B. G.; Lim, C.-H.; Miyake, G. M. Organocatalyzed Atom Transfer Radical Polymerization: Perspectives on Catalyst Design and Performance. *Macromol. Rapid Commun.* **2017**, *38*, 1700040.

(12) Discekici, E. H.; Anastasaki, A.; Read de Alaniz, J.; Hawker, C. J. Evolution and Future Directions of Metal-Free Atom Transfer Radical Polymerization. *Macromolecules* **2018**, *51*, 7421–7434.

(13) Dadashi-Silab, S.; Pan, X.; Matyjaszewski, K. Photoinduced Iron-Catalyzed Atom Transfer Radical Polymerization with ppm Levels of Iron Catalyst under Blue Light Irradiation. *Macromolecules* **2017**, *50*, 7967–7977.

(14) Kütahya, C.; Schmitz, C.; Strehmel, V.; Yagci, Y.; Strehmel, B. Near-Infrared Sensitized Photoinduced Atom-Transfer Radical Polymerization (ATRP) with a Copper(II) Catalyst Concentration in the ppm Range. *Angew. Chem., Int. Ed.* **2018**, *57*, 7898–7902.

(15) Treat, N. J.; Sprafke, H.; Kramer, J. W.; Clark, P. G.; Barton, B. E.; Read de Alaniz, J.; Fors, B. P.; Hawker, C. J. Metal-Free Atom Transfer Radical Polymerization. *J. Am. Chem. Soc.* **2014**, *136*, 16096–16101.

(16) Anastasaki, A.; Oschmann, B.; Willenbacher, J.; Melker, A.; Van Son, M. H. C.; Truong, N. P.; Schulze, M. W.; Discekici, E. H.; McGrath, A. J.; Davis, T. P.; Bates, C. M.; Hawker, C. J. One-Pot Synthesis of ABCDE Multiblock Copolymers with Hydrophobic, Hydrophilic, and Semi-Fluorinated Segments. *Angew. Chem., Int. Ed.* **2017**, *56*, 14483–14487.

(17) Konkolewicz, D.; Schröder, K.; Buback, J.; Bernhard, S.; Matyjaszewski, K. Visible Light and Sunlight Photoinduced ATRP with ppm of Cu Catalyst. *ACS Macro Lett.* **2012**, *1*, 1219–1223.

(18) Mosnáček, J.; Ilčíková, M. Photochemically Mediated Atom Transfer Radical Polymerization of Methyl Methacrylate Using ppm Amounts of Catalyst. *Macromolecules* **2012**, *45*, 5859–5865.

(19) Cole, J. P.; Federico, C. R.; Lim, C.-H.; Miyake, G. M. Photoinduced Organocatalyzed Atom Transfer Radical Polymerization Using Low ppm Catalyst Loading. *Macromolecules* **2019**, *52*, 747–754.

(20) Xu, J.; Jung, K.; Atme, A.; Shanmugam, S.; Boyer, C. A Robust and Versatile Photoinduced Living Polymerization of Conjugated and Unconjugated Monomers and Its Oxygen Tolerance. *J. Am. Chem. Soc.* **2014**, *136*, 5508–5519.

(21) Corrigan, N.; Shanmugam, S.; Xu, J.; Boyer, C. Photocatalysis in organic and polymer synthesis. *Chem. Soc. Rev.* **2016**, *45*, 6165–6212.

(22) Corrigan, N.; Yeow, J.; Judzewitsch, P.; Xu, J.; Boyer, C. Seeing the Light: Advancing Materials Chemistry through Photopolymerization. *Angew. Chem., Int. Ed.* **2019**, *58*, 5170–5189.

(23) Stache, E. E.; Kottisch, V.; Fors, B. P. Photocontrolled Radical Polymerization from Hydridic C–H Bonds. *J. Am. Chem. Soc.* **2020**, *142*, 4581–4585.

(24) Jiang, K.; Han, S.; Ma, M.; Zhang, L.; Zhao, Y.; Chen, M. Photoorganocatalyzed Reversible-Deactivation Alternating Copolymerization of Chlorotrifluoroethylene and Vinyl Ethers under Ambient Conditions: Facile Access to Main-Chain Fluorinated Copolymers. *J. Am. Chem. Soc.* **2020**, *142*, 7108–7115.

(25) Michaudel, Q.; Kottisch, V.; Fors, B. P. Cationic Polymerization: From Photoinitiation to Photocontrol. *Angew. Chem., Int. Ed.* **2017**, *56*, 9670–9679.

(26) Kottisch, V.; Supej, M. J.; Fors, B. P. Enhancing Temporal Control and Enabling Chain-End Modification in Photoregulated Cationic Polymerizations by Using Iridium-Based Catalysts. *Angew. Chem., Int. Ed.* **2018**, *57*, 8260–8264.

(27) Fu, C.; Xu, J.; Boyer, C. Photoacid-mediated ring opening polymerization driven by visible light. *Chem. Commun.* **2016**, *52*, 7126–7129.

(28) Ogawa, K. A.; Goetz, A. E.; Boydston, A. J. Metal-Free Ring-Opening Metathesis Polymerization. *J. Am. Chem. Soc.* **2015**, *137*, 1400–1403.

(29) Wang, J.-S.; Matyjaszewski, K. Controlled/“living” radical polymerization. atom transfer radical polymerization in the presence of transition-metal complexes. *J. Am. Chem. Soc.* **1995**, *117*, 5614–5615.

(30) Matyjaszewski, K.; Xia, J. Atom Transfer Radical Polymerization. *Chem. Rev.* **2001**, *101*, 2921–2990.

(31) Matyjaszewski, K.; Jakubowski, W.; Min, K.; Tang, W.; Huang, J.; Braunecker, W. A.; Tsarevsky, N. V. Diminishing catalyst concentration in atom transfer radical polymerization with reducing agents. *Proc. Natl. Acad. Sci. U.S.A.* **2006**, *103*, 15309–15314.

(32) Matyjaszewski, K. Atom Transfer Radical Polymerization (ATRP): Current Status and Future Perspectives. *Macromolecules* **2012**, *45*, 4015–4039.

(33) Matyjaszewski, K.; Tsarevsky, N. V. Macromolecular Engineering by Atom Transfer Radical Polymerization. *J. Am. Chem. Soc.* **2014**, *136*, 6513–6533.

(34) Matyjaszewski, K.; Coca, S.; Gaynor, S. G.; Wei, M.; Woodworth, B. E. Zerovalent Metals in Controlled/“Living” Radical Polymerization. *Macromolecules* **1997**, *30*, 7348–7350.

(35) Matyjaszewski, K.; Tsarevsky, N. V.; Braunecker, W. A.; Dong, H.; Huang, J.; Jakubowski, W.; Kwak, Y.; Nicolay, R.; Tang, W.; Yoon, J. A. Role of Cu0 in Controlled/“Living” Radical Polymerization. *Macromolecules* **2007**, *40*, 7795–7806.

(36) Konkolewicz, D.; Wang, Y.; Zhong, M.; Krys, P.; Isse, A. A.; Gennaro, A.; Matyjaszewski, K. Reversible-Deactivation Radical Polymerization in the Presence of Metallic Copper. A Critical Assessment of the SARA ATRP and SET-LRP Mechanisms. *Macromolecules* **2013**, *46*, 8749–8772.

(37) Anastasaki, A.; Nikolaou, V.; Nurumbetov, G.; Wilson, P.; Kempe, K.; Quinn, J. F.; Davis, T. P.; Whittaker, M. R.; Haddleton, D. M. Cu(0)-Mediated Living Radical Polymerization: A Versatile Tool for Materials Synthesis. *Chem. Rev.* **2016**, *116*, 835–877.

(38) Lorandi, F.; Fantin, M.; Isse, A. A.; Gennaro, A. RDRP in the presence of Cu0: The fate of Cu(1) proves the inconsistency of SET-LRP mechanism. *Polymer* **2015**, *72*, 238–245.

(39) Konkolewicz, D.; Magenau, A. J. D.; Averick, S. E.; Simakova, A.; He, H.; Matyjaszewski, K. ICAR ATRP with ppm Cu Catalyst in Water. *Macromolecules* **2012**, *45*, 4461–4468.

(40) Jakubowski, W.; Matyjaszewski, K. Activators Regenerated by Electron Transfer for Atom-Transfer Radical Polymerization of

(Meth)acrylates and Related Block Copolymers. *Angew. Chem., Int. Ed.* **2006**, *45*, 4482–4486.

(41) Costa, J. R. C.; Góis, J. R.; De Bon, F.; Serra, A. C.; Guliashvili, T.; Isse, A. A.; Gennaro, A.; Coelho, J. F. J. Addressing the role of triphenylphosphine in copper catalyzed ATRP. *Polym. Chem.* **2018**, *9*, 5348–5358.

(42) Tasdelen, M. A.; Uygun, M.; Yagci, Y. Photoinduced Controlled Radical Polymerization. *Macromol. Rapid Commun.* **2011**, *32*, 58–62.

(43) Ribelli, T. G.; Konkolewicz, D.; Bernhard, S.; Matyjaszewski, K. How are Radicals (Re)Generated in Photochemical ATRP? *J. Am. Chem. Soc.* **2014**, *136*, 13303–13312.

(44) Dadashi-Silab, S.; Atilla Tasdelen, M.; Yagci, Y. Photoinitiated atom transfer radical polymerization: Current status and future perspectives. *J. Polym. Sci., Part A: Polym. Chem.* **2014**, *52*, 2878–2888.

(45) Rolland, M.; Whitfield, R.; Messmer, D.; Parkatzidis, K.; Truong, N. P.; Anastasaki, A. Effect of Polymerization Components on Oxygen-Tolerant Photo-ATRP. *ACS Macro Lett.* **2019**, *8*, 1546–1551.

(46) Magenau, A. J. D.; Strandwitz, N. C.; Gennaro, A.; Matyjaszewski, K. Electrochemically Mediated Atom Transfer Radical Polymerization. *Science* **2011**, *332*, 81–84.

(47) Chmielarz, P.; Fantin, M.; Park, S.; Isse, A. A.; Gennaro, A.; Magenau, A. J. D.; Sobkowiak, A.; Matyjaszewski, K. Electrochemically mediated atom transfer radical polymerization (eATRP). *Prog. Polym. Sci.* **2017**, *69*, 47–78.

(48) Lorandi, F.; Fantin, M.; Isse, A. A.; Gennaro, A. Electrochemical triggering and control of atom transfer radical polymerization. *Curr. Opin. Electrochem.* **2018**, *8*, 1–7.

(49) Li, B.; Yu, B.; Huck, W. T. S.; Liu, W.; Zhou, F. Electrochemically Mediated Atom Transfer Radical Polymerization on Nonconducting Substrates: Controlled Brush Growth through Catalyst Diffusion. *J. Am. Chem. Soc.* **2013**, *135*, 1708–1710.

(50) Mohapatra, H.; Kleiman, M.; Esser-Kahn, A. P. Mechanically controlled radical polymerization initiated by ultrasound. *Nat. Chem.* **2016**, *9*, 135.

(51) Wang, Z.; Pan, X.; Yan, J.; Dadashi-Silab, S.; Xie, G.; Zhang, J.; Wang, Z.; Xia, H.; Matyjaszewski, K. Temporal Control in Mechanically Controlled Atom Transfer Radical Polymerization Using Low ppm of Cu Catalyst. *ACS Macro Lett.* **2017**, *6*, 546–549.

(52) Wang, Z.; Lorandi, F.; Fantin, M.; Wang, Z.; Yan, J.; Wang, Z.; Xia, H.; Matyjaszewski, K. Atom Transfer Radical Polymerization Enabled by Sonochemically Labile Cu-carbonate Species. *ACS Macro Lett.* **2019**, *8*, 161–165.

(53) Zhou, Y.-N.; Li, J.-J.; Ljubic, D.; Luo, Z.-H.; Zhu, S. Mechanically Mediated Atom Transfer Radical Polymerization: Exploring Its Potential at High Conversions. *Macromolecules* **2018**, *51*, 6911–6921.

(54) Dadashi-Silab, S.; Lorandi, F.; Fantin, M.; Matyjaszewski, K. Redox-switchable atom transfer radical polymerization. *Chem. Commun.* **2019**, *55*, 612–615.

(55) Dadashi-Silab, S.; Matyjaszewski, K. Temporal Control in Atom Transfer Radical Polymerization Using Zerovalent Metals. *Macromolecules* **2018**, *51*, 4250–4258.

(56) Dolinski, N. D.; Page, Z. A.; Discekici, E. H.; Meis, D.; Lee, I. H.; Jones, G. R.; Whitfield, R.; Pan, X.; McCarthy, B. G.; Shanmugam, S.; Kottisch, V.; Fors, B. P.; Boyer, C.; Miyake, G. M.; Matyjaszewski, K.; Haddleton, D. M.; Alaniz, J. R.; Anastasaki, A.; Hawker, C. J. What happens in the dark? Assessing the temporal control of photo-mediated controlled radical polymerizations. *J. Polym. Sci., Part A: Polym. Chem.* **2019**, *57*, 268–273.

(57) Dadashi-Silab, S.; Matyjaszewski, K. Iron-Catalyzed Atom Transfer Radical Polymerization of Semifluorinated Methacrylates. *ACS Macro Lett.* **2019**, *8*, 1110–1114.

(58) Krys, P.; Matyjaszewski, K. Kinetics of Atom Transfer Radical Polymerization. *Eur. Polym. J.* **2017**, *89*, 482–523.

(59) Ribelli, T. G.; Fantin, M.; Daran, J.-C.; Augustine, K. F.; Poli, R.; Matyjaszewski, K. Synthesis and Characterization of the Most Active Copper ATRP Catalyst Based on Tris[(4-dimethylaminopyridyl)methyl]amine. *J. Am. Chem. Soc.* **2018**, *140*, 1525–1534.

(60) Ribelli, T. G.; Lorandi, F.; Fantin, M.; Matyjaszewski, K. Atom Transfer Radical Polymerization: Billion Times More Active Catalysts and New Initiation Systems. *Macromol. Rapid Commun.* **2019**, *40*, 1800616.

(61) Whitfield, R.; Parkatzidis, K.; Rolland, M.; Truong, N. P.; Anastasaki, A. Tuning Dispersity by Photoinduced Atom Transfer Radical Polymerisation: Monomodal Distributions with ppm Copper Concentration. *Angew. Chem., Int. Ed.* **2019**, *58*, 13323–13328.

(62) Lorandi, F.; Matyjaszewski, K. Why Do We Need More Active ATRP Catalysts? *Isr. J. Chem.* **2020**, *60*, 108–123.

(63) Fischer, H. The Persistent Radical Effect: A Principle for Selective Radical Reactions and Living Radical Polymerizations. *Chem. Rev.* **2001**, *101*, 3581–3610.

(64) Fantin, M.; Isse, A. A.; Bortolamei, N.; Matyjaszewski, K.; Gennaro, A. Electrochemical approaches to the determination of rate constants for the activation step in atom transfer radical polymerization. *Electrochim. Acta* **2016**, *222*, 393–401.

(65) Dolinski, N. D.; Page, Z. A.; Eisenreich, F.; Niu, J.; Hecht, S.; Read de Alaniz, J.; Hawker, C. J. A Versatile Approach for In Situ Monitoring of Photoswitches and Photopolymerizations. *ChemPhotoChem* **2017**, *1*, 125–131.

(66) Dong, H.; Matyjaszewski, K. ARGET ATRP of 2-(Dimethylamino)ethyl Methacrylate as an Intrinsic Reducing Agent. *Macromolecules* **2008**, *41*, 6868–6870.

(67) Kwak, Y.; Matyjaszewski, K. ARGET ATRP of methyl methacrylate in the presence of nitrogen-based ligands as reducing agents. *Polym. Int.* **2009**, *58*, 242–247.

(68) Braunecker, W. A.; Tsarevsky, N. V.; Gennaro, A.; Matyjaszewski, K. Thermodynamic Components of the Atom Transfer Radical Polymerization Equilibrium: Quantifying Solvent Effects. *Macromolecules* **2009**, *42*, 6348–6360.

(69) Lorandi, F.; Fantin, M.; Isse, A. A.; Gennaro, A.; Matyjaszewski, K. New protocol to determine the equilibrium constant of atom transfer radical polymerization. *Electrochim. Acta* **2018**, *260*, 648–655.

(70) Isse, A. A.; Bortolamei, N.; De Paoli, P.; Gennaro, A. On the mechanism of activation of copper-catalyzed atom transfer radical polymerization. *Electrochim. Acta* **2013**, *110*, 655–662.

(71) Buback, M.; Kurz, C. H.; Schmaltz, C. Pressure dependence of propagation rate coefficients in free-radical homopolymerizations of methyl acrylate and dodecyl acrylate. *Macromol. Chem. Phys.* **1998**, *199*, 1721–1727.

(72) Ribelli, T. G.; Augustine, K. F.; Fantin, M.; Krys, P.; Poli, R.; Matyjaszewski, K. Disproportionation or Combination? The Termination of Acrylate Radicals in ATRP. *Macromolecules* **2017**, *50*, 7920–7929.

(73) Ribelli, T. G.; Wahidur Rahaman, S. M.; Daran, J.-C.; Krys, P.; Matyjaszewski, K.; Poli, R. Effect of Ligand Structure on the CuII–R OMNP Dormant Species and Its Consequences for Catalytic Radical Termination in ATRP. *Macromolecules* **2016**, *49*, 7749–7757.

(74) Wulkow, M. Computer Aided Modeling of Polymer Reaction Engineering—The Status of Predici, I-Simulation. *Macromol. React. Eng.* **2008**, *2*, 461–494.

(75) Fantin, M.; Lorandi, F.; Ribelli, T. G.; Szczepaniak, G.; Enciso, A. E.; Fliedel, C.; Thevenin, L.; Isse, A. A.; Poli, R.; Matyjaszewski, K. Impact of Organometallic Intermediates on Copper-Catalyzed Atom Transfer Radical Polymerization. *Macromolecules* **2019**, *52*, 4079–4090.

(76) Thevenin, L.; Fliedel, C.; Fantin, M.; Ribelli, T. G.; Matyjaszewski, K.; Poli, R. Reductive Termination of Cyanoisopropyl Radicals by Copper(I) Complexes and Proton Donors: Organometallic Intermediates or Coupled Proton–Electron Transfer? *Inorg. Chem.* **2019**, *58*, 6445–6457.